eJSE International

Electronic Journal of Structural Engineering (10) 2010

Probabilistic Analysis and Optimization of Roof Trusses

A. Olsson*
School of Engineering, Linnaeus University, Växjö, Sweden
Email: anders.olsson@lnu.se

ABSTRACT: The influence of gap between wooden members and displaced nail-plates in roof trusses is investigated by means of probabilistic calculations and structural optimization. The employed mechanical model, using the finite element method, captures the non-linear behaviour of the nail-plate joints. The joint stiffness involves the size and location of the nail-plate, and the presence of contact or gap respectively between the wooden members. The analysis shows that even small initial gaps considerably increase the deflection of a roof truss. Misplaced nail-plates also effect the deflection negatively, but it is also shown that the deflection can be significantly decreased, and the utilization of nail-plates improved, by optimizing the nail-plate positions with respect to critical load cases and requirements.

1 INTRODUCTION

Wooden roof trusses with nail-plate joints are widely employed in modern roof construction. In Sweden, for example, roof trusses with nail-plate joints constitute the main load-carrying system of the roof structure in more than 50% of all residential buildings. This large volume makes a detailed understanding of the mechanical behaviour of these structures urgent, as it is necessary in order to secure a satisfactory safety and serviceability of the structures and to achieve an optimal use of resources in terms of material consumption and manufacturing control.

In addition to a detailed mechanical modelling of ideal roof trusses and nail-plate joints it is important to consider uncertainties in material properties and in geometrical imperfections. Such uncertainties may significantly effect the stiffness and load-carrying capacity of wooden roof trusses. Variations in stiffness and strength of wood material have been studied by several researchers, e.g. Isaksson (1999), and probabilistic models for wood have been applied on roof trusses, aiming at a better understanding of the actual safety levels (Hansson 2001). Research with a probabilistic outlook on geometrical imperfections in nail-plate joints have, however, to the knowledge of the author, not been carried out before. The present paper is a result of ongoing research on roof truss modelling and geometrical imperfections. It presents models and calculations on the influence of misplaced nail-plates and gap between wooden members in roof trusses. The research also aims at development and comparison of methods for probabilistic analysis and optimization, that can be efficiently employed in conjunction with non-linear finite element models of roof trusses and structural systems in general.

2 MODELLING OF ROOF TRUSSES

2.1 *Overview of methods*

In commercial software for roof truss analysis the nail-plate joints are typically regarded as either rigid or pin-ended and the wooden members are modelled by beam elements with a linear elastic behaviour. Several such models have been collected and evaluated by Petersson and Olsson (1994) and Olsson and Rosenqvist (1996). In reality, however, nail-plate joints have complicated stiffness properties. The load-deformation relation cannot be expected to behave linearly and when approaching the limit-state loading the failure of a joint, and thereby the entire truss, may be caused by different phenomena such as fracture in the wooden members, pull-out behaviour of the nails or buckling of the nail-plates. Thus, this type of modelling only gives rough predictions of failure or unacceptable deformations through indirect criteria specified by

structural codes. The codes in turn must rely on more advanced models and calculations in combination with laboratory tests.

Linear and non-linear elastic models considering joint deformations have also been developed. Foschi (1977) presented a model for nail-plate joints, able to capture the nail stiffness for different orientations in relation to the loading and wood fibre direction. It was also able to capture local plate buckling, and gap or contact respectively between wooden members. The key work by Foschi has been followed by further development, modifications and software development (e.g. Petersson and Olsson 1994; Olsson and Rosenqvist 1996; Nielsen 1996; Berglund and Holmberg 2000; Ellegaard 2001).

More advanced models, using 2D or 3D finite elements, plasticity theory and fracture mechanics, must be employed in order to capture the nail-plate joint behaviour in detail when loaded until failure. Some work in this area has also been carried out (e.g. Nielsen 1996 and Kevarinmäki 2000) but these models have only been employed on single joints and are primarily suitable for research on details in the mechanical behaviour of joints and for calibration of simplified joint models.

Our purpose is to investigate the impact of gap between wooden members, and the influence of randomly misplaced nail-plates, on the deformations of roof trusses. This requires a large number of runs and it is therefore important that a single deterministic calculation can be carried out at a low computational cost. The Foschi type model fulfills our requirements and a simple version of it will be employed herein. The following presentation of the mechanical model is similar to the presentation and model by Nielsen (1996) although it differs in some details.

2.2 *A non-linear model for nail-plate joints*

A roof truss can be divided in nail-plate joints and wooden members between the joints. The wooden members between the joints are modelled herein by Timoshenko beam elements which are located in the system lines. The wooden members are assumed to behave linearly elastic.

The joints are modelled by three different types of elements, namely; nail elements, splice elements and contact elements. A nail element represents the nails of a plate area fastened into one wooden member. The splice element represents the plate covering the border between two wooden members. It is connected, in the model, to two nail elements. The splice element captures the normal and shear deformations of the plate. The contact element is used to capture the contact pressure between wooden members. Gap between wooden members may be initially present due to tolerances and fabrication errors but contact may arise as a consequence of the roof truss deformation when loaded. It is required, of course, that an initial gap is closed in order to put the contact element into action. Finally, rigid connections are employed in the model too. These are used to couple other elements and transfer forces and moments due to the geometry of the joint and the model. Figure 1 shows an arbitrary nail-plate joint and the elements used in the modelling. Below follows the derivations of the element stiffness matrices of the joint elements.

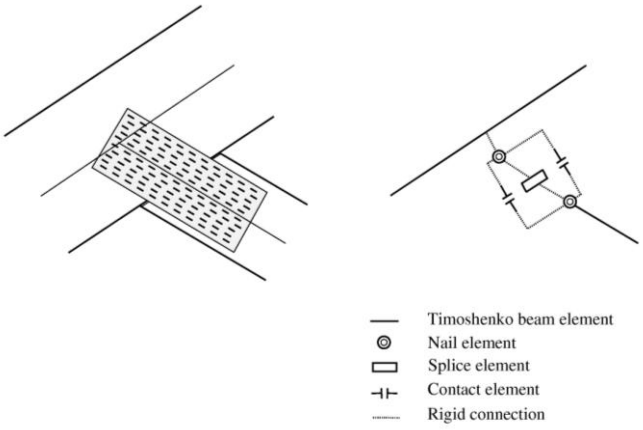

Figure 1: Nail-plate joint and corresponding mechanical model. Different element symbols are introduced.

2.2.1 *The nail element*

Each nail of the nail-plate area contribute to the stiffness of the corresponding nail element. The contribution of a nail to the rotational stiffness is dependent of the distance to the rotational centre. This is captured by the distance to the nodal points of the nail element, i.e. to the reference positions in the wooden and nail-plate parts respectively. An important assumption is that the plate area and the corresponding wooden area of the nail element transform and rotate rigidly, i.e. do not deform. Figure 2 shows the local coordinate system of a nail element along with the global coordinate system of the model. It also shows the nodal points of the nail element and the position of an arbitrary location i in the nail-plate area. Thus, even though the nail element symbol introduced in Figure 1 indicates that both nodes of the element are located at the same position this is only one possible choice. The node positions may be chosen arbitrarily.

The absolute displacement between the wood and the plate in point i of the nail-plate area is calculated as

$$\Delta = \sqrt{\Delta_x^2 + \Delta_y^2} \tag{1}$$

where Δ_x and Δ_y are the displacements in the x-direction and in the y-direction respectively, calculated as

$$\Delta_x = \mathbf{q}_x^T \mathbf{u}^{(n)}; \quad \Delta_y = \mathbf{q}_y^T \mathbf{u}^{(n)} \tag{2}$$

where, with reference to Figure 2,

$$\mathbf{q}_x = [1 \; 0 \; -(y_i - y_w) \; -1 \; 0 \; (y_i - y_p)]^T \tag{3}$$

$$\mathbf{q}_y = [0 \; 1 \; (x_i - x_w) \; 0 \; -1 \; -(x_i - x_p)]^T \tag{4}$$

$$\mathbf{u}^{(n)} = [u_w \; v_w \; w_w \; u_p \; v_p \; w_p]^T \tag{5}$$

The displacement between two arbitrary points, in the plate and in the wood respectively, can thus be uniquely determined by the translations and rotations of the nodal points.

The stiffness relation adopted in the model, Eq. 6, was suggested by Foschi (1977).

$$p(\Delta) = (p_0 + k_1\Delta)\left(1 - exp\left(\frac{-k_0\Delta}{p_0}\right)\right) \tag{6}$$

The force, p, on a tooth in position i is a function of the absolute displacement between the plate and the wood, Δ, and three stiffness parameters. These parameters, p_0, k_0 and k_1, can be estimated by means of laboratory tests. The parameters may be functions of the angle between the grain direction of the wood and the principal axis of the plate, and of the direction of the force transmitted by the nail (Foschi 1977). In our simplified version of the model, however, and in accordance with Nielsen (1996), the stiffness parameters are assumed to be independent of directions. Figure 3 illustrates the force-displacement curve and shows the significance of p_0, k_0 and k_1 in the model.

The secant and tangent stiffness matrices of the nail element, in the local coordinate system, can now be established. The reader may consult Nielsen (1996) for details in the derivation of the secant stiffness matrix using the principle of virtual work. Only the resulting expression is presented herein. The secant stiffness matrix, $K_s^{(n)}$, can be expressed as

$$\mathbf{K}_s^{(n)} = \int_A \Im \frac{p(\Delta)}{\Delta} (q_x q_x^T + q_y q_y^T) dA \tag{7}$$

where $\Im$ is the nail density, i.e the number of nails per unit area, and A is the nail-plate area represented by the nail element.

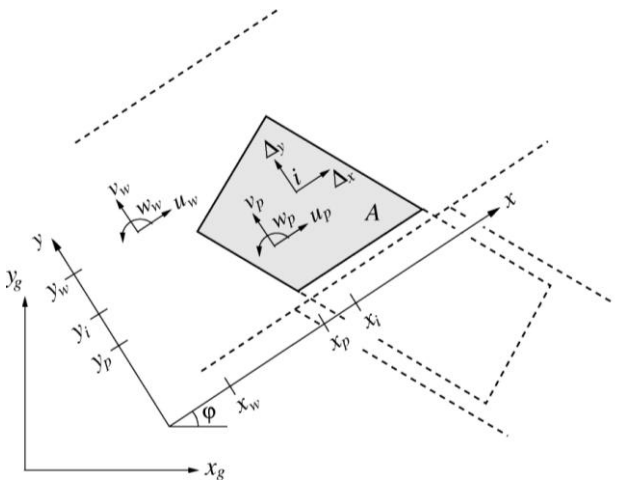

Figure 2: Global and local coordinate systems of a nail element and delimitations of the corresponding nail-plate area. The degrees of freedom of the node of the plate are denoted $[u_p, v_p, w_p]$ and the degrees of freedom of the node of the wood are denoted $[u_w, v_w, w_w]$.

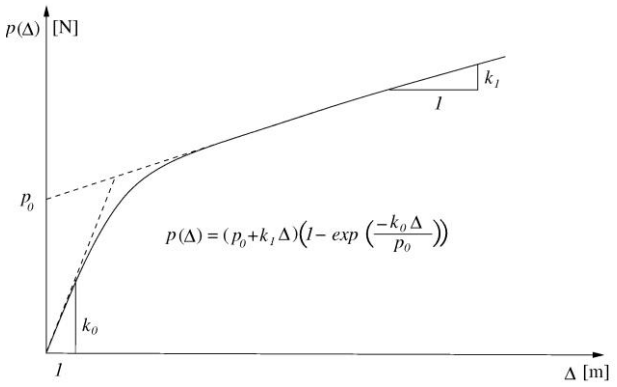

Figure 3: Force-displacement relation for one nail of the plate area represented by the nail element, and definitions of the model stiffness parameters.

As a typical nail element comprises a large number of nails it is practical to consider the nails and their stiffness contributions as smeared over the plate area and thus calculate the stiffness matrix of a nail element by numerical integration over the plate area of the element. The tangent stiffness matrix, $K_t^{(n)}$, is finally expressed as

$$\mathbf{K}_t^{(n)} = \int_A \Im \frac{\partial p(\Delta)}{\partial \Delta} (q_x q_x^T + q_y q_y^T) dA \tag{8}$$

2.2.2 *The splice element*

The splice element is used to model the plate area close to the splice between two wooden members. The teeth are ineffective in this area because they are located between the wooden members or very close to the edges of the wooden members. As the teeth are cut out from the plate the remaining, perforated plate area, shaded in Figure 4, consists of a network

of approximately rectangularly formed small pieces. In the models presented by Foschi (1977) and Nielsen (1996) the plate area of the splice element was modelled by a number of beam elements representing the plate material between the holes. In the present model the stiffness of the splice element is captured by adopting a non-linear spring stiffness $[\mathrm{N/m^2}]$ in the x-direction and in the y-direction respectively along the splice, see Figure 4. This approach has an advantage as the stiffness is smeared over the length of the splice and is thereby continuous. The beam approach, on the other hand, represents the splice by a discrete number of small beams. This difference is important when it comes to probabilistic calculations and optimization of the structure later on.

As the adjacent plate areas represented by the nail elements are assumed to be rigid, the displacement of each point, along the borders of the splice element, $x_\alpha \le x \le x_\beta$ and $y = y_1$ or $y = y_2$, see Figure 4, is uniquely determined by the translations and rotations of the nodal points of the splice element. The locations of the nodal points, a and b, are arbitrary.

The kinematic relation between the nodal points and the positions along the edges of the splice area is expressed by

$$\bar{\mathbf{u}} = \mathbf{D}\mathbf{u}^{(s)} \tag{9}$$

where

$$\bar{\mathbf{u}} = \begin{bmatrix} u_1 & v_1 & w_1 & u_2 & v_2 & w_2 \end{bmatrix}^T \tag{10}$$

$$\mathbf{u}^{(s)} = \begin{bmatrix} u_a & v_a & w_a & u_b & v_b & w_b \end{bmatrix}^T \tag{11}$$

and, with $x = x_1 = x_2$,

$$\mathbf{D} = \begin{bmatrix} 1 & 0 & y_a - y_1 & & & \\ 0 & 1 & x - x_a & \mathbf{0} & & \\ 0 & 0 & 1 & & & \\ & & & 1 & 0 & y_b - y_2 \\ & \mathbf{0} & & 0 & 1 & x - x_b \\ & & & 0 & 0 & 1 \end{bmatrix} \tag{12}$$

In correspondence with the displacement vectors, $\mathbf{u}^{(s)}$ and $\mathbf{u}$, force vectors are defined by $\mathbf{f}^{(s)}$ and $f dx$. The force components and moment components of $\bar{\mathbf{f}}^{(s)}$ correspond to the translation directions and rotations of $\mathbf{u}^{(s)}$ and the components of $\bar{\mathbf{f}}$ correspond in the same way to the components of $\bar{\mathbf{u}}$. The vector $\mathbf{f}^{(s)}$ is related to $\bar{\mathbf{f}}$ as

$$\mathbf{f}^{(s)} = \int_{x=x_\alpha}^{x_\beta} \mathbf{D}^T \bar{\mathbf{f}} dx \tag{13}$$

and the relation between $\bar{\mathbf{f}}$ and $\bar{\mathbf{u}}$ is expressed by

$$\bar{\mathbf{f}} = \bar{\mathbf{K}}\bar{\mathbf{u}} \tag{14}$$

where

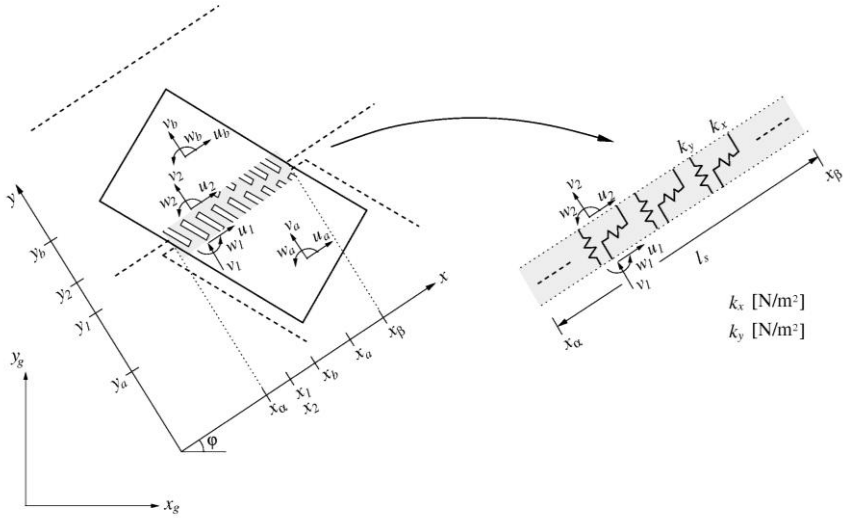

Figure 4: Geometry, degrees of freedom and coordinate systems of a splice element. The degrees of freedom of the nodal points are denoted $[u_a, v_a, w_a]$ and $[u_b, v_b, w_b]$ respectively, and the translations and rotations in some position along the splice are denoted $[u_1, v_1, w_1]$ and $[u_2, v_2, w_2]$ respectively.

$$\overline{\mathbf{K}} = \begin{bmatrix} k_x & 0 & 0 & -k_x & 0 & 0 \\ 0 & k_y & 0 & 0 & -k_y & 0 \\ 0 & 0 & 0 & 0 & 0 & 0 \\ -k_x & 0 & 0 & k_x & 0 & 0 \\ 0 & -k_y & 0 & 0 & k_y & 0 \\ 0 & 0 & 0 & 0 & 0 & 0 \end{bmatrix} \quad [N/m^2] \quad (15)$$

The parameters k_x and k_y are the spring stiffness of the splice element, in the x-direction and y-direction respectively, per unit length along the splice. By inserting Eqs. 9 and 14 into Eq. 13 the local finite element equation is established by

$$\mathbf{f}^{(s)} = \mathbf{K}^{(s)}\mathbf{u}^{(s)} \quad (16)$$

where the stiffness matrix, $\mathbf{K}^{(s)}$, is given by

$$\mathbf{K}^{(s)} = \int_{x=x_\alpha}^{x_\beta} \mathbf{D}^T \overline{\mathbf{K}} \mathbf{D} dx \quad (17)$$

The spring stiffness, k_x and k_y, must finally be supplied to the model and a bilinear relation between stiffness and displacement is adopted herein, see Figure 5. As for the nail element, the secant stiffness matrix as well as the tangent stiffness matrix are derived, but as a general expression for the stiffness matrix is already given, Eq. 17, it only remains to supply values for k_x and k_y for the two alternative stiffness matrices. However, even though the values of the parameters in the x-direction and in the y-direction may differ, the same procedure is employed for the derivation of k_x and k_y. Therefore, only the derivation of k_x is presented below. (k_y can be derived by replacing index x by index y in Eqs. 18-20). For the secant stiffness matrix the value assigned to k_x is

$$k_x = \frac{k_x^0 c_x^c + k_x^c(\delta_x - c_x^c)}{\delta_x}, \qquad \delta_x < c_x^c$$

$$k_x = k_x^0, \qquad c_x^c \le \delta_x \le c_x^t \quad (18)$$

$$k_x = \frac{k_x^0 c_x^t + k_x^t(\delta_x - c_x^t)}{\delta_x}, \qquad \delta_x > c_x^t$$

and for the tangent stiffness matrix the values assigned to k_x is

$$k_x = k_x^c, \qquad \delta_x < c_x^c$$

$$k_x = k_x^0, \quad c_x^c \le \delta_x \le c_x^t \quad (19)$$

$$k_x = k_x^t, \qquad \delta_x > c_x^t$$

where δ_x is the displacement defined by

$$\delta_x = u_2(x) - u_1(x) \quad (20)$$

The parameters k_x^c, k_x^0, k_x^t, c_x^c and c_x^t are defined by Figure 5 and should be determined by means of laboratory tests.

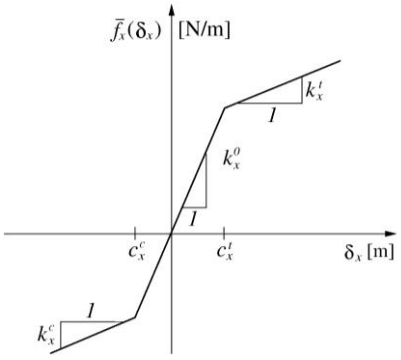

Figure 5: Bi-linear spring stiffness in the x-direction. c_x^c and c_x^t indicate critical displacements for which the tangent stiffness changes. The tangent stiffness for different displacements, δ_x, is represented by k_x^c, k_x^0 and k_x^t respectively.

2.2.3 *The contact element*

Contact pressure between wooden members arise in different locations of the roof truss when it is loaded, unless the initial gaps between the wooden members are too large. Contact elements should therefore be added to the model in locations where contact pressure may arise. Figure 6 shows the locations of two contact elements capturing the potential contact pressure between two wooden members. A contact element may be coupled to the beam elements of the wooden members by auxiliary beam elements or by geometrical transformations directly to the nodes of the beam elements representing the wooden members. The stiffness matrix of a contact element is derived below with respect to the degrees of freedom located where the contact takes place.

The important parameters of a contact element are; the initial gap size between the wooden members, the normal stiffness of the contact element when put into action and the coefficient of friction between the wooden members.

The element displacement vector is defined, with reference to Figure 6, as

$$\mathbf{u}^{(c)} = \begin{bmatrix} v_A & v_A & u_B & v_B \end{bmatrix}^T \quad (21)$$

The criterion for contact between the wooden members at the location of the element is

$$v_A - v_B \ge g \quad (22)$$

where g is the initial gap size. The element stiffness matrix of the contact element can, in the local coordinate system, be expressed as

$$\mathbf{K}^{(c)} = \begin{bmatrix} k_f & 0 & -k_f & 0 \\ 0 & k_n & 0 & -k_n \\ -k_f & 0 & k_f & 0 \\ 0 & -k_n & 0 & k_n \end{bmatrix} \quad [N/m] \qquad (23)$$

where k_n is the normal stiffness perpendicular to the edges of the two wooden members and k_f is the shear stiffness caused by friction between the wooden members. k_f is a function of the normal force and the coefficient of friction. In the following derivations herein, however, friction is neglected giving $k_f = 0$.

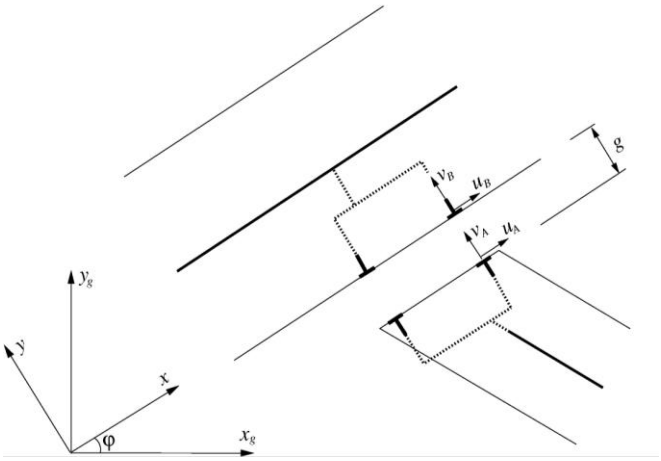

Figure 6: Contact elements for modelling of contact pressure between wooden members.

The element equation in local coordinates can be expressed as

$$\mathbf{f}^{(c)} = \mathbf{K}^{(c)}\mathbf{u}^{(c)} \qquad (24)$$

where the four components of the force vector, $\mathbf{f}^{(c)}$, correspond to the four components of the displacement vector, $\mathbf{u}^{(c)}$.

The remaining task is to determine the value of the normal stiffness component, k_n, of $\mathbf{K}^{(c)}$. As before, the tangent as well as the secant stiffness matrices will be considered. The tangent and secant stiffness respectively, k_t and k_s, are indicated in Figure 7. For the tangent stiffness matrix, k_n is given by

$$k_n = k_t = 0, \qquad d < g \qquad (25)$$

$$k_n = k_t = \frac{EA_c}{L}, \quad d \geq g$$

where d is the current relative displacement, $v_A - v_B$. E is the modulus of elasticity of the wood material, which depends on the angles between the fibre directions of the wooden members and the contact surface. A_c is the estimated area of the contact surface between the members represented by the contact element, and L is the length of the wood material in contact pressure modelled by the contact element. It may be noted that the estimated parameters E, A_c and L are only employed in order to find a physical foundation for the estimation of the stiffness $k_s(d \geq g)$. If $k_s(d \geq g)$ can be estimated by laboratory experiments, E, A_c and L are not needed.

The secant stiffness, k_s, is a function of the tangent stiffness parameter, k_t, and the initial gap size, g. For the secant stiffness matrix, k_n is defined by

$$k_n = k_s = 0, \qquad d < g \qquad (26)$$

$$k_n = k_s = \frac{k_t(d-g)}{d}, \quad d \geq g$$

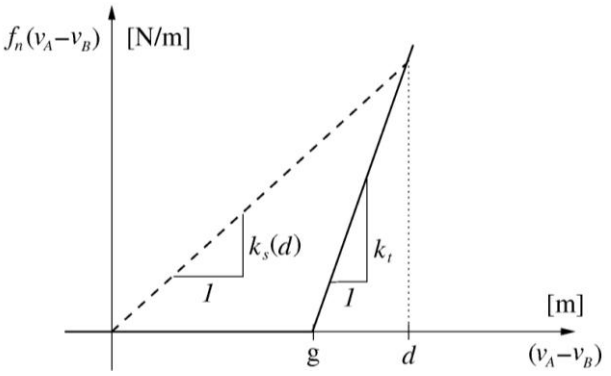

Figure 7: Contact force, f_n, as function (solid line) of relative displacement and initial gap size. The tangent stiffness, k_t, and the secant stiffness, k_s, are illustrated. d is the current relative displacement.

2.3 *Application on a roof truss*

The elements presented are now employed in the analysis of a complete roof truss using the software MATLAB (2002) and the finite element toolbox CALFEM (1999). The considered roof truss is a common symmetric W-truss with a roof angle of 20^o and a span of approximately eight meters. The geometry of the truss and the nail-plate joints is shown in Figure 8, and the mechanical model of the joints, using the element symbols defined in Figure 1, is presented in Figure 9. The same truss was analyzed by Nielsen (1996) and some material properties for the nail-plate joints are collected from his work.

Table 1 states the parameters of the truss elements. The first column contains the stiffness parameters of the wooden members. E_0 is the modulus of elasticity in the fibre direction and E_{90} is the modulus of elasticity in direction perpendicular to the fibre direction. G is the shear modulus. These wood parameters could be chosen differently depending on strength class, load duration and climate conditions for the structure. For our purposes, however, i.e. to calculate the influence of geometrical imperfection, it is sufficient to choose realistic stiffness values for the wooden members and not define under which precise conditions the chosen values are valid. Column two and column tree of Table 1 states the parameters of the nail elements and the splice elements respectively. The parameters originate to the plate type *GNA20S* produced by the company *MiTek* and the given values are valid for single nail-plates. As nail-plates are present on both sides of the wooden members of the truss, double nail elements and splice elements are assembled in the model.

The normal, tangent stiffness of the contact elements in action depends on the estimated contact area, A_c, the estimated length of the contact zone, L, and the modulus of elasticity of the wood in compression, E, which is highly dependent on the angle between the contact pressure and the wood fibre direction. The employed stiffness of each contact element, $k_t = EA_c/L$, is, with reference to the contact element numbering of Figure 9, supplied in the fourth column of Table 1.

Two different load cases are considered in the present study. Load case A, shown in Figure 10, represents a realistic loading in relation to the design of the truss. Load case B is simply twice the loading of load case A. Load case B is hardly realistic for the truss under consideration, but it is useful for studying the effects of geometrical imperfections when the joints are heavily loaded.

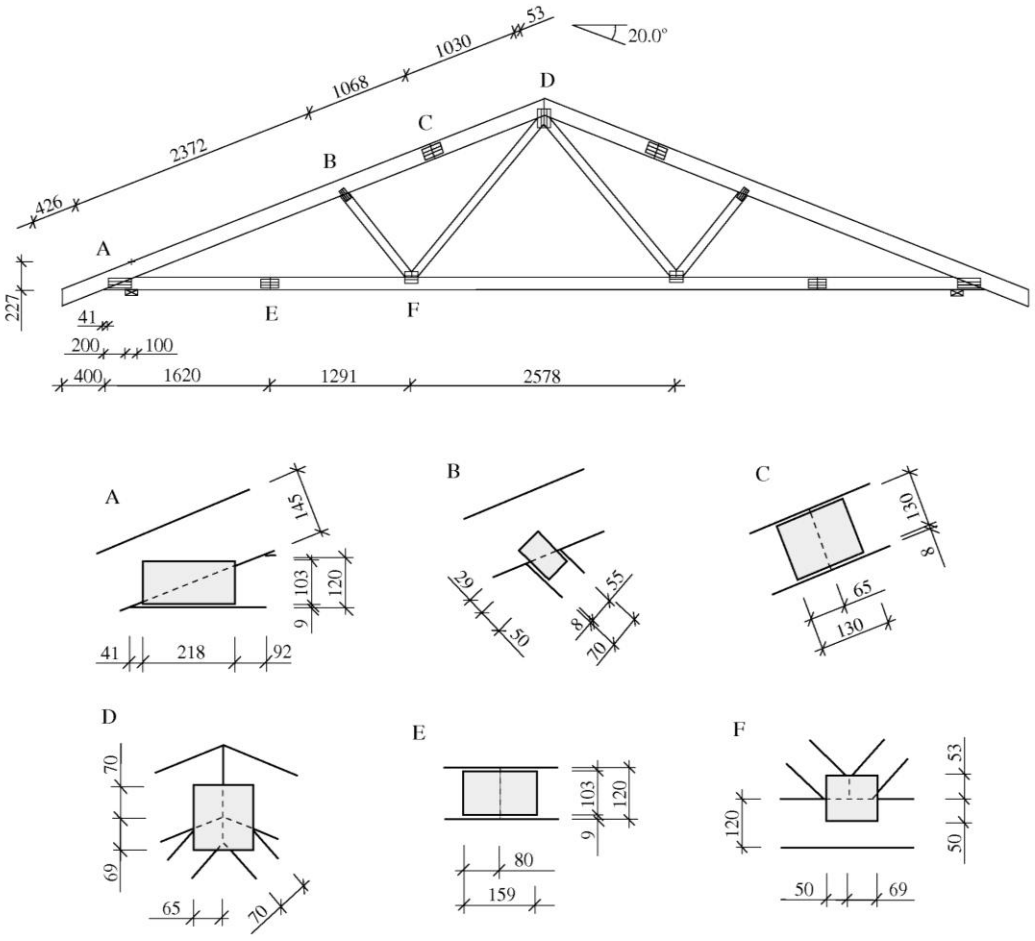

Figure 8: Geometry of a symmetric, 20^o, W-truss including the nail-plate locations. Lengths are given in mm.

Table 1: Parameters of the truss elements. The first column contains the stiffness parameters of the wooden members. The second and third columns state the parameters of the nail elements and the splice elements respectively, and the fourth column states the normal stiffness of the contact elements.

Wooden members	Nail element par.	Splice element par.	Contact stiffness
$E_0 = 7200\,\text{MPa}$	$p_0 = 150\,\text{N}$	$k_x^c = 3.44\,\text{MN/m}^2$	(1) $k_t = 14.5\,\text{MN/m}$
$E_{90} = 240\,\text{MPa}$	$k_0 = 900\,\text{N/m}^2$	$k_x^0 = 183\,\text{MN/m}^2$	(2) $k_t = 29.5\,\text{MN/m}$
$G = 480\,\text{MPa}$	$k_1 = 80\,\text{kN/m}$	$k_x^t = 3.44\,\text{MN/m}^2$	(3a) $k_t = 295\text{MN/m}$
	$\mathfrak{I} = 14650\text{teeth/m}^2$	$k_y^c = 86.8\,\text{MN/m}^2$	(3b) $k_t = 295\text{MN/m}$
		$k_y^0 = 4630\,\text{MN/m}^2$	(4a) $k_t = 254\text{MN/m}$
		$k_y^t = 86.8\,\text{MN/m}^2$	(4b) $k_t = 254\text{MN/m}$
		$c_x^c = -2.0\times10^{-4}\,\text{m}$	(5) $k_t = 15.1\text{MN/m}$
		$c_x^t = 2.0\times10^{-4}\,\text{m}$	
		$c_y^c = -4.4\times10^{-5}\,\text{m}$	
		$c_y^t = 4.4\times10^{-5}\,\text{m}$	

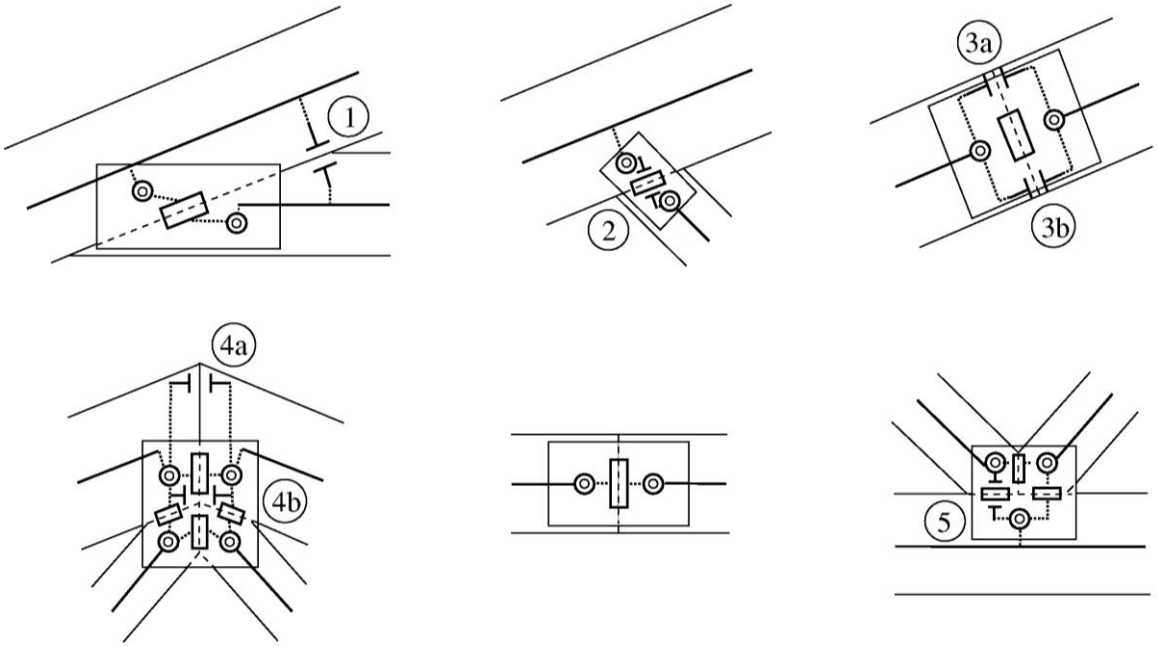

Figure 9: Mechanical model of the nail-plate joints using nail elements, splice elements and contact elements. The numbering refers to the contact elements.

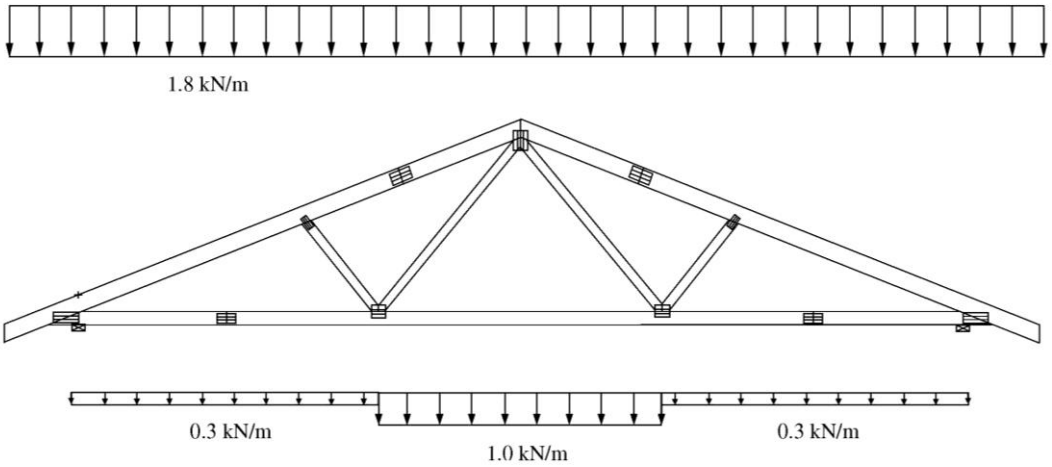

Figure 10: Definition of load case A.

2.3.1 *Results*

The results presented herein are restricted to the deflection of the truss. The deflection supplies a measure of the overall stiffness of the truss, and requirements on the deflection are often critical for the design of roof trusses.

The maximum deflection of the truss under consideration takes place in the middle of the chord. This is indicated in Figure 11, which shows the deformation mode of the entire truss for load case A. The relation between the deflection of the middle of the chord and the applied loading is shown in Figure 12. The different curves represent cases with; initial contact between the wooden members, no contact between the wooden members, and rigid nail-plate connections. The stiffness curve representing the rigid connection model shows that a substantial part of the deflection depends on the limited stiffness of the wooden members, modelled by Timoshenko beams. Otherwise the deflection for this model would be smaller. However, even though the stiffness of the nail-plate joints is relatively high, the presence of contact between the wooden members makes a significant contribution to the overall stiffness compared to the case without any contact between the wooden members. Lack of contact also results in a more pronounced non-linear behaviour as larger deformations are reached in the nail-plate joints.

Depending on the load level, the maximum deflection of the truss differs about $15-25\%$ for models with initial contact compared to models without any contact between wooden members. For load case A, the deflection is 18.6 mm in case of initial contact and 21.3 mm in case of no contact. For load case B, the deflections are 38.9 mm and 48.4 mm for initial contact and no contact respectively. In reality, initial gap may close as a result of deformations in the nail-plate joints subjected to loading. Large initial gap, however, may not close for any realistic loading on the roof truss and the magnitude of the initial gap is therefore of vital importance for the overall stiffness and deformation of the truss.

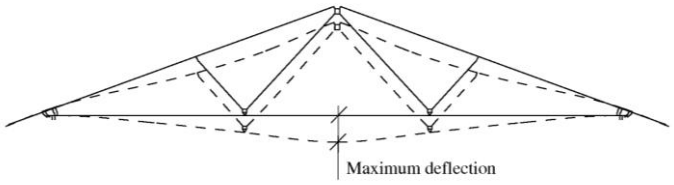

Figure 11: Deformation mode of the W-truss, with initial contact between wooden members, subjected to load case A. The deformation is shown with a magnification factor of twenty.

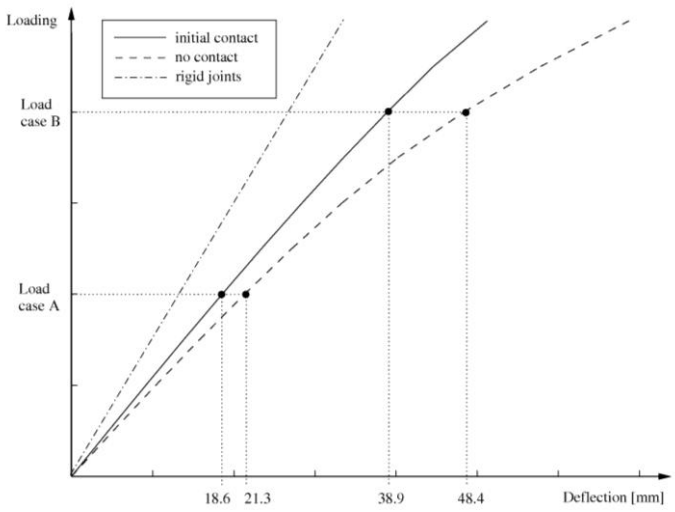

Figure 12: The relation between loading and deflection for cases with initial contact between wooden members, and no contact between wooden members, respectively. The stiffness curve of a roof truss model with rigid joints is also presented.

3 GEOMETRICAL IMPERFECTIONS

3.1 *Gap between wooden members*

The computational results presented above comprise the case of initial contact between all pairs of wooden members, and the case of no contact between any wooden members. Below follows a parameter study on gaps at different locations and a probabilistic analysis on the influence of randomly distributed gaps in a roof truss.

3.1.1 *Parameter study on the effect of gap*

For each pair of wooden members, for which contact as well as gap are possible and have influence on the behaviour of the truss, the effects of gap of different magnitudes are investigated. Table 2 and Table 3 state, for load cases A and B respectively, the relative increase in deflection of the roof truss for gap of different magnitudes and at different locations. The numbering, 1-5, corresponds to the contact location numbering of Figure 9. For those joints modelled by more than one contact element (joint 3 and 4) the same initial gap size is assumed to be present throughout the splice. In each case of Tables 2-3, initial contact between wooden members is assumed at all other locations of the roof truss.

The most important location, with respect to contact vs gap, is joint 4, at the top of the roof truss. An initial gap here results in an increase in deflection of at most for load case A, and for load case B. For load case B, however, the initial gap must be almost 4 mm wide in order to remain unclosed when the entire load is applied, whereas for load case A, an initial gap of 1 mm remains unclosed. An initial gap of 1 mm gives, for load case B, an increase in deflection of 3.5%.

Table 2: For load case A, influence of gap of different magnitudes at different positions where contact matters. The values given are the ratio between the deflection of the truss with a certain gap, and the deflection of the truss with initial contact.

Gap size	1	2	3(a–b)	4(a–b)	5
0.25 mm	1.003	0.999	1.012	1.019	1.015
0.50 mm	1.006	0.999	1.013	1.036	1.025
1.00 mm	1.006	0.999	1.013	1.055	1.025
1.50 mm	1.006	0.999	1.013	1.055	1.025

Table 3: For load case B, influence of gap of different magnitudes at different positions where contact matters. The values given are the quota between the deflection of the truss with a certain gap, and the deflection of the truss with initial contact.

Gap size	1	2	3(a–b)	4(a–b)	5
0.25 mm	1.002	0.999	1.007	1.010	1.007
0.50 mm	1.003	0.999	1.012	1.018	1.015
1.00 mm	1.007	0.999	1.020	1.035	1.028
1.50 mm	1.008	0.999	1.020	1.054	1.028
2.00 mm	1.008	0.999	1.020	1.073	1.028
4.00 mm	1.008	0.999	1.020	1.106	1.028

Gap at joint 2 actually decreases, though not significantly, the deflection of the chord. This result may surprise at a first glance, but the deflection of the middle of the chord does not capture the complete behaviour of the truss. For example, gap at joint 2 also results in increased deflection of the rafter for the same load cases.

In contrast to gap at joint 2, gap at joint 5, at the opposite end of the short diagonal wooden member, has a significant and increasing effect on the deflection. It is actually the second most important contact location after the top joint. The reason for this is that gap/contact at joint 5 has direct impact on the internal forces and the deformations of the entire nail plate connecting the chord and the two diagonal members. Gap at joint 5 thus increases the internal forces and the deformations of the adjacent nail and splice elements, coupled to the chord and the longer diagonal.

Joint 3, the splice joint of the rafter, is sensitive even to small gap. An initial gap of 0.25 mm in this single joint results in, for load case A, an increase of the deflection of 1.2%.

Gap at joint 5, the heel joint, does not have a major effect on the deflection. The reasons for this are that the contact element is relatively weak as it models wood in compression in the weak direction parallel to the fibre direction, and that friction between wooden members is ignored. Also, the size of the nail plate at the heel joint is quite large, giving a stiff connection and only small relative displacements of the wooden members in the direction perpendicular to the contact surface. Therefore, the additional effect of contact between the chord and the rafter is moderate.

For load case A, no initial gap of more than 1 mm closes during loading. Thus, the deflection for a case with gap above 1 mm coincides with a case where contact is ignored. For load case B larger gaps are closed during loading, but when the initial gap size is increased above a certain level this has no impact, according to the model, on the behaviour of the roof truss. The reason for this is that the employed model does not capture phenomena such as buckling of the nail plates, caused by large gap, as the stiffness of the splice elements are not sensitive to the gap size. Therefore, the present model, and consequently also the results, are not valid for very large gaps. However, in contrast to commercial software using very simple mechanical models, the employed model al-

lows the required modifications at a reasonable additional effort.

3.1.2 *Probabilistic analysis on the influence of gap*

The presence of gaps in manufactured roof trusses is a consequence of lack of precision, and possibly lack of control, in the manufacturing process. Gaps are therefore randomly distributed and a roof truss may contain several gaps of different magnitudes at different joint locations. A proper analysis on the influence of gap must therefore involve probabilistic calculations, where the presence of gap is modelled by statistical distributions. These distributions should rely on thorough investigations on the actual gap magnitudes present in manufactured roof trusses. Unfortunately, however, no such investigation is available at this point. Instead we must make reasonable assumptions, and rely on these assumptions in the following calculations.

Four different distributions of the initial gap sizes are considered. In each case a uniform distribution is assumed and the intervals are $[0:0.25]$, $[0:0.5]$, $[0:1.0]$ and $[0:1.5]$ mm respectively. In total, nine pairs of wooden members are modelled by twelve contact elements, see Figure 9 (not showing joints represented by their reversed joints). No correlation or dependence is assumed between the gap sizes at different locations within the roof truss.

The probabilistic analysis is performed using Monte Carlo simulations and the Latin hypercube sampling plan. The Latin hypercube sampling plan, first proposed by McKay et al. (1979), is more efficient than standard Monte Carlo sampling as it represents the distributions of the input data, in this case the gap magnitudes, accurately with a reasonable sample size. The method has been further developed for different purposes by several researchers [e.g Owen (1994); Olsson and Sandberg (2001)] and has been evaluated for structural mechanics applications by Olsson (1999).

The results of the probabilistic analysis are shown in Figure 13 and Figure 14 for load cases A and B respectively. The histograms, comprising one thousand deterministic calculations each, show the distributions of the roof-truss deflection (the deflection of the middle of the chord) for the four different distributions of the gap magnitude. The deflections for the extreme cases, with initial contact and no contact between wooden members respectively, are marked by dashed lines in the histograms. The deflections for the cases with initial gap sizes equal to the upper limits of the distributions (0.25, 0.5, 1.0 and 1.5 mm respectively) are marked in the histograms by dotted lines.

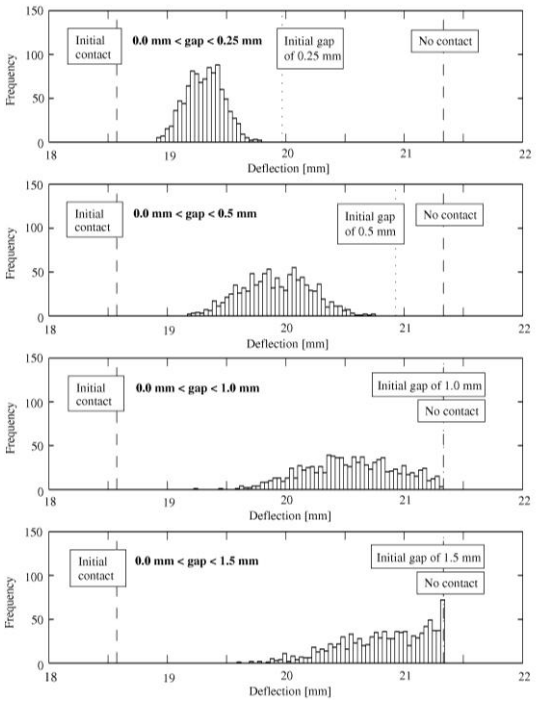

Figure 13: Histograms of the roof-truss deflection corresponding to load case A, and four different uniform distributions of the gap magnitude.

It is clear from Figures 13-14 that even small initial gap, gap < 0.25 mm, significantly effect the deflection of the truss. For initial gap sizes equal to 0.25 mm the deflection is increased by 7.5% and 4.0%, for load cases A and B respectively, compared to the truss with initial contact. It is interesting to note, that for load case A, small gap results in a larger relative increase of the deflection than for load case B. Gap larger than approximately 1 mm, on the other hand, have larger impact on the deflection for load case B.

The probabilistic results presented by the histograms give useful information on the probability for a certain deflection to be exceeded. However, without going into details about exact probabilities, it is clear that for each gap distribution and each load case, there is a significant risk that the deflection comes close to the upper bound of that particular case, i.e close to the dotted line in the histogram. For load case A, assuming the wide gap intervals of $[0:1.0]$ and $[0:1.5]$ mm, it seems even reasonable to neglect contact between wooden members when calculating the deflection.

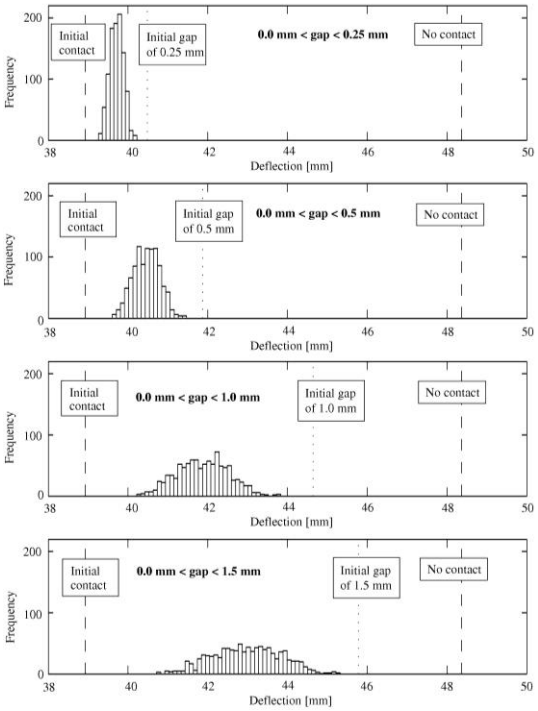

Figure 14: Histograms of the roof-truss deflection corresponding to load case B, and four different uniform distributions of the gap magnitude.

It is finally concluded that a thorough investigation on the actual presence of gap in roof trusses would be most interesting in order to establish a valid statistical distribution of the gap magnitude. It would also be very interesting to study, by means of laboratory tests and advanced finite element calculations, the behaviour in bending and compression of nail plate joints when large gaps between wooden members are present. Such an investigation would probably imply a sensitivity to the gap size in the properties of the splice element.

3.2 *Location of nail-plates*

In contrast to models frequently employed in industry, the model employed herein captures the exact nail-plate location when calculating the deformations. Thus, we are able to investigate the effects of changes in the nail-plate locations. Displacements of nail-plates in relation to the prescribed locations may occur as a result of lack of precision in the manufacturing process and it is investigated how such random misplacement influences the behaviour of the roof truss. Another aspect considered is the possibility to improve the roof truss behaviour with respect to some critical criterion, in this case the deflection of the middle of the chord, by performing an optimization procedure on the nail-plate locations.

Nail-plates are located on both sides of the wooden members and this is modelled, as before, by double nail and splice element stiffness. Thus, the plates on the opposite sides of the wooden members (with identical $xy-$coordinates) are restricted, in the present model, to move in the same way.

3.2.1 *Probabilistic analysis on misplaced nail-plates*

In similarity with the analysis on gap between wooden members, a probabilistic analysis on misplaced nail-plates is carried out. The probability distribution of the misplacement of the nail-plates should, preferably, be founded on a thorough investigation on actual nail-plate locations of manufactured roof trusses. As no such investigation is available the employed distribution of misplacement is instead founded on typical tolerances for nail-plate locations. A misplacement of at most 5 mm is often accepted and a uniform distribution in the interval $[-5:5]$ mm is therefore adopted herein for the misplacement in the length direction and cross direction respectively of each nail-plate.

The probabilistic analysis is performed using Monte Carlo simulations and the Latin hypercube sampling plan. Cases with initial contact between wooden members as well as without any contact between wooden members are considered, and simulations are carried out for load cases A and B respectively. For each of the four combinations a probabilistic analysis consisting of one thousand deterministic calculations is carried out. The resulting deflections of the middle of the chord are visualized by the histograms in Figures 15-16.

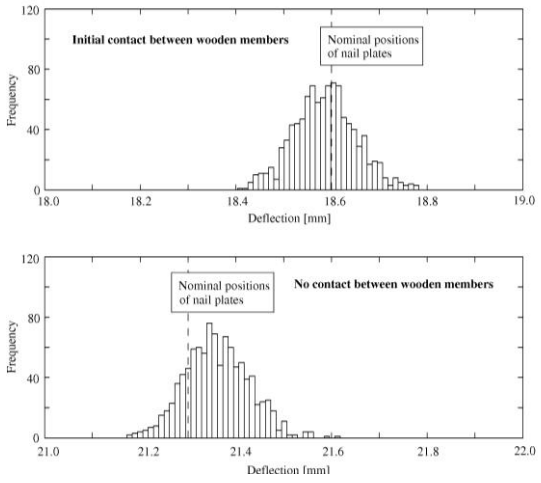

Figure 15: Histograms of the roof-truss deflection corresponding to load case A, and uniformly distributed displacements of nail-plates, $[-5:5]$ mm. Cases with initial contact and no contact between wooden members respectively are presented.

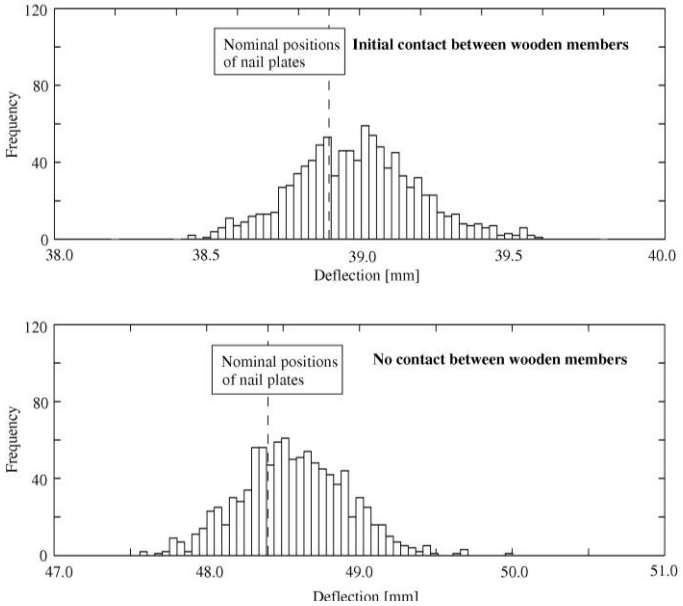

Figure 16: Histograms of the roof-truss deflection corresponding to load case B, and uniformly distributed displacements of nail-plates, $[-5:5]$ mm. Cases with initial contact and no contact between wooden members respectively are presented.

The distributions of the roof truss deflection appears, in all the cases, to be approximately normally distributed with a moderate standard deviation. Of course, however, the intervals between the largest and smallest possible defections are limited as the nail-plate displacements are moderate and limited. It is also clear from Figures 15-16 that the influence of misplaced nail-plates is larger for roof trusses without contact between wooden members than for roof trusses with initial contact, and larger for load case B than for load case A. For load case B and no contact between wooden members the difference between the smallest and largest deflection is about 5%, or 2.5 mm deflection. For load case A and initial contact the difference is only about 2%, or 0.5 mm deflection. The reason for this is that for load case B the nail-plates are heavily loaded and have lower tangent stiffness. Small changes in positions, therefore, give large impact on the deformation. Also, in case of no contact between wooden members the nail-plates constitute the only load carriers between the wooden members, and the overall stiffness and deformation of the truss are more sensitive to changes of the nail-plate positions than if contact is present.

The deflection for the case with nominal positions of the nail-plates are marked in Figures 15-16 and it is obvious that the nominal nail-plate positions do not result in minimal deflection of the middle of the chord. For all four cases considered, a significant part of the random nail-plate configurations give lower deflections than the nominal configuration. This observation turns our interest towards an optimization of the nail-plate positions with respect to the deflection.

3.2.2 *Optimization of nail-plate positions*

It is fundamental for all optimization that a certain function of the involved variables is defined for evaluation. In the present case, the selected function is the deflection of the middle of the chord. The goal is to find the nail-plate configuration that minimizes this deflection. The displacements of the nail-plates in length direction and cross direction, see Figure 17, are thus the variables determining the deflection.

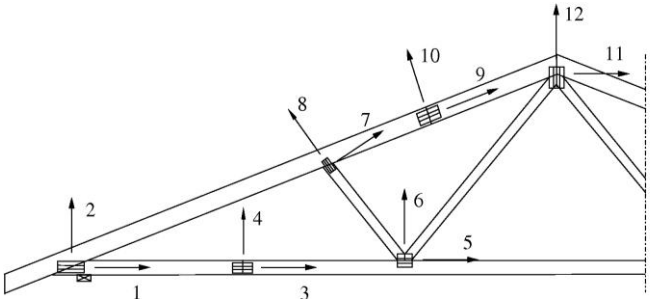

Figure 17: Left part of the roof truss with definition and numbering of displacement directions of the nail-plates.

Different constraints, i.e. restrictions on the optimization variables, may be applied in the search for the optimal solution. In the present case restrictions are placed on the displacements of the nail-plates. For example, the plate connecting the chord with the two diagonal wooden members is not allowed to be moved more than 5 mm in its length and cross direction respectively. The reason for this is that an extreme displacement of this nail-plate, towards loss of connection between the short diagonal and the other wooden members, would be favourable for the deflection under consideration, for the present load cases. It is easy to realize, however, that such a displacement would be far from optimal with respect to other demands on the roof truss and for other load cases.

The analysis comprises the four cases considered in the investigation on misplaced nail-plates, i.e with and without contact between wooden members, and load cases A and B respectively. The resulting optimal nail-plate displacement, with reference to the variable numbering of Figure 17, are presented in Tables 4-5, for load cases A and B respectively, along with the corresponding deflections of the middle of the chord. Displacements restricted by constraints are marked by a (C) in Tables 4-5.

Table 4: Nail-plate displacements, in relation to the initial positions, giving minimum deflection of the chord of the roof truss for load case A. Activated constraints are indicated by (C). The resulting reductions of the deflection are also supplied.

	Initial contact	No contact
Displacement	Load case A	Load case A
1	1.9 mm	2.4 mm
2	-3.9 mm	-0.5 mm
3	-0.1 mm	-0.1 mm
4	9.0 mm (C)	9.0 mm (C)
5	5.0 mm (C)	5.0 mm (C)
6	5.0 mm (C)	4.3 mm
7	0.6 mm	1.0 mm
8	-0.1 mm	-0.1 mm
9	0.1 mm	0.1 mm
10	9.0 mm (C)	9.0 mm (C)
11	0.0 mm	0.0 mm
12	-5.0 mm (C)	5.8 mm
Reduction of deflection	1.6%	1.7%

Table 5: Nail-plate displacements, in relation to the initial positions, giving minimum deflection of the chord of the roof truss for load case B. Activated constraints are indicated by (C). The resulting reductions of the deflection are also supplied.

	Initial contact	No contact
Displacement	Load case B	Load case B
1	2.2 mm	3.2 mm
2	-4.4 mm	-0.6 mm
3	-0.1 mm	-0.2 mm
4	9.0 mm (C)	9.0 mm (C)
5	5.0 mm (C)	5.0 mm (C)
6	5.0 mm (C)	3.4 mm
7	0.3 mm	0.4 mm
8	-0.1 mm	-0.1 mm
9	0.1 mm	0.2 mm
10	9.0 mm (C)	9.0 mm (C)
11	0.0 mm	0.0 mm
12	-5.0 mm (C)	7.3 mm
Reduction of deflection	2.4%	3.8%

According to the calculations the optimum location for the nail-plate at the heel joint is fairly close to the nominal position. A moderate displacement to the right and downwards is, however, favourable for decreasing the deflection. This holds for all four cases considered, but the exact optimal displacement differs somewhat for the different cases. No constraints are activated at the heel joint.

The nail-plates at the splice joints, connecting the wooden members of the chord and the rafter respectively, are moved towards the upper edges of the wooden members. For all cases considered the best location is such that the upper edge of the nail-plates coincide with the upper edges of the wooden members. This is a reasonable result knowing that the maximum tension at the splice joint of the chord, as well as the maximum compression at the splice joint of the rafter, are located at the upper edges. It is assumed herein that the nails remain effective even if they are located close to the edges of the wood. It should also be noted that a different load case could give maximum tension at the lower edge of the splice joint of the chord, which would result in a nail-plate displacement towards the lower edge at this joint.

The nail-plate connecting the chord with the two diagonal members of the roof truss is moved upwards and towards increased connection between the chord and the long diagonal member. The displacement of the nail-plate is limited by constraints allowing only 5 mm displacements in the length and cross directions of the plate.

The optimal position of the nail-plate at the top joint depends on the presence of contact between the two rafters. In case of initial contact the plate is displaced downwards, increasing the connection between the long diagonal elements of the roof truss and the rafters. The two rafters are connected by contact pressure in combination with the nail-plate. On the other hand, in the cases of no contact between the wooden members the nail-plate is displaced upwards. In this case the nail-plate is moved towards a stiffer connection between the rafters.

The results of the optimization procedure with respect to the target function, the deflection of the middle of the chord, are also presented in Table 5. The reduction of the deflection is $1.6-3.8\%$, compared to the deflection with nominal nail-plate positions, where the higher value is valid for load case B in case of no contact between wooden members. This reduction is modest, but significant. In the design of a roof truss there is often a critical deflection for one load case that may not be exceeded. If calculations, considering a preliminary design, show that the allowed deflection will be exceeded it may be a solution to perform optimization on the nail-plate positions aiming at decreased deflection. This is of course an attractive option compared to increasing the dimensions of wooden members and nail-plates.

3.2.3 *The optimization procedure*

Finally, a few comments on the optimization procedure should be supplied. A traditional optimization procedure using the steepest decent method is employed. In brevity, starting at the nominal nail-plate positions, the gradient of the target function, i.e. the deflection, is calculated with

respect to the nail-plate displacements. Then the quadratic fit method is employed. The target function is evaluated at two additional locations along the direction of the calculated gradient, giving that the deflection is known at three different locations, and that a quadratic polynomial can be fitted to these values. The polynomial in turn suggests a new position along the gradient direction for which the target function is minimized (according to the quadratic approximation). Then a new gradient is calculated at this new position and the procedure proceeds with a new quadratic fit and so on. The procedure is a common strategy in structural optimization and a textbook on the subject is written by Luenberger (1989).

An important detail in the implementation of the present optimization problem is the calculations of gradients. The gradient is calculated numerically, and a general perturbation procedure, for calculating the gradient once, would require a complete calculation of the deflection for twenty-two different nail-plate configurations (as the truss has eleven nail-plates, each with two displacement degrees of freedom). However, as the non-linear model is elastic, i.e the response is path independent, the gradient can be calculated by only performing one additional increment, and not a complete solution, for each of the twenty-two nail-plate displacements. This feature is very important for the computational efficiency giving that the optimization procedure can be carried out at a very low computational cost, namely the cost of solving the problem for one nail-plate configuration, times three (for the quadratic fit), times the number of iterations for convergence (about five or ten). The strategy for effective calculations of gradients in non-linear elastic problems is presented in detail by Liu and Der Kiureghian (1991).

4 CONCLUDING REMARKS AND FURTHER RESEARCH

An investigation on the influence of geometrical imperfections in roof trusses has been carried out using a non-linear model able to consider the stiffness of nail-plate joints including contact pressure between wooden members.

Gap between wooden members, compared to initial contact between members, was found to be of great importance for the deflection and overall stiffness of the considered 20^o W-truss. For moderate loading the deflection of the middle of the chord was about 15% larger for the case without contact, and the difference was even larger for higher loading. It was also found that small initial gaps between wooden members, less than 0.5 mm, distributed at different locations in the truss, result in a significant impact on the deflection.

Further work on gap between wooden members should comprise a thorough investigation on actual gap sizes present in manufactured roof trusses. Also, laboratory tests on nail-plate joints in order to calibrate stiffness properties of nail-plates and contact pressure should be carried out. In particular, the friction coefficients for different wood fibre directions, and the influence of the butt effect should be evaluated and considered in the calculations. The butt effect is the effect that sawn surfaces of wood, pressed into each other in the fibre direction, tend to have a relatively low initial contact stiffness. Moreover, the splice elements of the mechanical model should be modified, according to laboratory tests, to be able to capture the effects of very large gaps between wooden members. Such gaps could be catastrophic for the behaviour of the truss. In addition, the dependence on the angle between the plate direction and the splice direction should be evaluated and considered for the stiffness parameters of the splice element. Finally, not only stiffness and deformations should be considered in the evaluations, but also the ultimate strength of roof trusses.

Misplaced nail-plates may have negative effect on the stiffness and deflection of the roof truss. However, if the misplacement magnitudes are moderate, less than 5 mm, the influence on the deflection is much smaller than the influence of gap between wooden members. Controlled displacements of nail-plates, on the other hand, can be used in order to improve the behaviour of the roof truss. It was shown that the deflection can be reduced by about $2-4\%$, depending on the load case and the presence of contact. Moreover, it was shown that the employed non-linear and elastic mechanical model can, at a low computational cost, be combined with an optimization procedure adapted for the problem.

One type of geometrical imperfection, not considered herein, is poorly pressed nail-plates. Such nail-plates have reduced stiffness and strength and the problem should be considered in a way similar to the types of geometrical imperfections treated herein, in combination with laboratory work.

The conclusions from research on geometrical properties of wooden roof trusses with nail-plate joints can be used for development of more accurate and complete computer software than those employed in industry today. The suggested models and routines can be used not only to increase the

safety and performance of roof trusses, but also to improve the utilization of material, components and tolerances in industry.

REFERENCES

Berglund, P. and Holmberg, J., (2000), ``CALROOF - Program for Modelling of Roof Trusses Considering Flexibility of Joints," Rep. TVSM-5099, Division of Struct. Mech., Lund Univ., Lund, Sweden, (in Swedish).

CALFEM, (1999), ``A finite element toolbox to MATLAB, Version 3.3" Rep. TVSM-9001, Division of Struct. Mech., Lund Univ., Lund, Sweden.

Ellegard, P., (2001), ``Analysis of Timber Joints With Punched Metal Plate Fasteners - With Focus on Knee Joints," ISSN 1395-7953 R0206, Dept. of Build. Techn. and Struct. Eng., Aalborg Univ., Aalborg, Denmark.

Foschi, R., (1977), ``Analysis of Wood Diaphragms and Trusses, Part II: Truss-plate Connections," Can. J. Civ. Eng., 4, 353–362.

Hansson, M., (2001), ``Reliability of Timber Structural Systems," Rep. TVBK-1022, Division of Struct. Eng., Lund Univ., Lund, Sweden.

Isaksson, T., (1999), ``Modelling the Variability of Bending Strength in Structural Timber," Rep. TVBK-1015, Division of Struct. Eng., Lund Univ., Lund, Sweden.

Kevarinmäki, A., (2000), ``Semi-Rigid behaviour of Nail-plate Joints," Rep. TKK-TRT-109, Lab. of Struct. Eng., Helsinki Univ. of Tech., Espoo, Finland.

Liu, P.-L. and Der Kiureghian A., (1991), ``Finite Element Reliability of Geometrically Nonlinear Uncertain Structures," J. Eng. Mech., 117, 1806–1825.

Luenberger, D. (1989), ``Linear and Nonlinear Programming," Addison-Wesley Publication Company, Menlon Park, California.

MATLAB, (2002), ``High-performance numerical computation and visualization software, Version 6.1", The Math Works Inc, Natic Ma.

McKay, M. D., Conover, W. J., and Beckman R.J. (1979), ``A Comparison of Three Methods for Selecting Values of Input Variables in the Analysis of Output from a Computer Code," Technometrics, 21, 239–245.

Nielsen, J., (1996), ``Stiffness Analysis of Nail-plate Joints Subjected to Short-term Loads," ISSN 1395-7953 R9613, Dept. of Build. Techn. and Struct. Eng., Aalborg Univ., Aalborg, Denmark.

Olsson, A. and Rosenqvist, F., (1996), ``Comparative Calculations of Deflections in Wooden Roof-trusses Connected with Nail-plates," Rep. TVSM-5066, Division of Struct. Mech., Lund Univ., Lund, Sweden, (in Swedish).

Olsson, A., and Sandberg, G. (2001), ``On Latin Hypercube Sampling for Stochastic Finite Element Analysis," J. Eng. Mech., 128, 121–125.

Owen, A. B. (1994), ``Controlling Correlations in Latin Hypercube Samples," J. American Stat. Ass., 89, 1517–1522.

Petersson, H. and Olsson, K.-G., (1994), ``Simple Models for Roof Truss Analysis," Proc. of COST C1 Workshop, Prague, Czech Republic.

Olsson, A., (1999), ``Modelling Damage and Stochastic Properties in Engineering Structures," Rep. TVSM-3037, Division of Struct. Mech., Lund Univ., Lund, Sweden.